ION CHANNELS, RECEPTORS AND TRANSPORTERS

Role of bestrophin-1 in store-operated calcium entry in retinal pigment epithelium

Néstor Más Gómez · Ernst R. Tamm · Olaf Strauβ

Abstract The retinal pigment epithelium (RPE) expresses bestrophin-1 where mutant bestrophin cause retinal degenerations. Overexpression of bestrophin-1 demonstrated Ca^{2+}-dependent Cl^- channel function, whereas the RPE in bestrophin-1 knockout or mutant bestrophin-1 knock-in mice showed no change in Cl^- conductance. To account for these apparently mutually exclusive findings, we investigated the function of endogenously expressed bestrophin-1 in a short-time RPE cell culture system by means of immunocytochemistry, Ca^{2+} imaging, and siRNA knockdown. Immunocytochemical quantification of bestrophin-1 localization demonstrated 2.5 times higher co-localization with the endoplasmic reticulum (ER) Ca^{2+}-sensor protein, Stim-1, than with the membrane protein β-catenin, implicating it in store-operated Ca^{2+} entry (SOCE). Ca^{2+} release from ER stores under extracellular Ca^{2+}-free conditions using thapsigargin (1 μM) to inhibit endoplasmic Ca^{2+} ATPase (SERCA) followed by re-adjustment of extracellular Ca^{2+} to physiological levels activated SOCE, which was insensitive to the blocker of numerous transient receptor potential channels and voltage-dependent Ca^{2+} channels SKF96563 (1 μM). SOCE was augmented at 5 μM and inhibited at 75 μM by 2-aminoethoxydiphenyl borate which indicates the involvement Orai-1 channels. In confirmation, SOCE was decreased by siRNA knockdown of Orai-1 expression. SOCE amplitude was strongly reduced by siRNA knockdown of bestrophin-1 expression, which was due to neither changes in Stim-1/Orai-1 expression nor Stim-1/bestrophin-1 interaction. The amount of Ca^{2+} released by SERCA inhibition was reduced after siRNA knockdown of bestrophin-1, but not of Orai-1. In conclusion we found that a proportion of bestrophin-1 is functionally localized to ER Ca^{2+} stores where it influences the amount of Ca^{2+} and therefore Ca^{2+} signals which result from activation of Orai-1 via Stim-1.

Keywords Bestrophin-1 · Endoplasmic reticulum Ca^{2+} store · Orai-1 · Store-operated calcium entry

N. M. Gómez · O. Strauβ (✉)
Experimental Ophthalmology, Eye Hospital, University Medical Center Regensburg, Franz-Josef-Strauss-Allee 11,
93053 Regensburg, Germany
e-mail: strauss@eye-regensburg.de

E. R. Tamm
Institute of Human Anatomy and Embryology,
University of Regensburg, Regensburg, Germany

Introduction

The retinal pigmented epithelium (RPE) has a variety of functions which are essential to maintain structural integrity and excitability of photoreceptors [7, 40, 41]. Many of these functions are controlled by increases in cytosolic free Ca^{2+} [45]. Since the functional interaction between RPE cells and photoreceptors is indispensable for visual function, impaired RPE function leads to photoreceptor degeneration [14, 16, 26]. Thus the understanding of Ca^{2+}-dependent regulation of RPE cell function will also help to clarify pathomechanisms of diseases leading to blindness.

Bestrophin-1 is the gene product of the *BEST1* gene which is expressed in RPE cells [33]. *BEST1* mutations lead to various types of retinal degeneration such as Best's vitelliform macular dystrophy, an inherited autosomal dominant form of macular degeneration [24]. Characteristic of Best's disease is an early accumulation of lipofuscin in the RPE and the reduction of the light peak in the electro-oculogram (EOG) [2, 44]. In overexpression studies, bestrophin-1 was found to have a double function, as a chloride channel and a modulator of calcium signaling [34, 36, 42, 48]. Overexpression studies have shown that bestrophin-1 can regulate L-type channel activity through interaction between proline-

rich motifs on its C-terminal and SH3-domains of β-subunits of L-type channels [28, 34]. The light peak in the EOG is dependent on the activity of Cl⁻ channels in the RPE basolateral membrane and of L-type Ca^{2+} channels. Thus, the reduced light peak in Best's patients could possibly arise from a disturbed bestrophin-1 Ca^{2+} channel interaction [10, 23, 36] which is supported by observations in $Ca_V1.3$ or Ca^{2+} channel β4-subunit knockout mice models where the light peak is reduced [23, 46]. On the other hand, the reduction of the light peak in Best patients could also be explained by a loss Cl⁻ channel function of bestrophin-1 [42]. Since bestrophin-1 localizes basolaterally in RPE cells and the light peak seems to be generated by increases in Cl⁻ conductance across the basolateral membrane, it could be that bestrophin-1 provides the underlying Cl⁻ conductance [22]. However, RPE cells of bestrophin-1 knockout mice or $Best^{W93C/W93C}$ knock-in mice (one of the mutations found in Best patients) showed no differences in the Cl⁻ conductance compared to wild-type mice. In addition, bestrophin-1 knockout mice showed increased light peaks in the DC-ERG. These observations challenge the function of bestrophin-1 as a plasma membrane Cl⁻ channel [23, 52].

Studies of endogenously expressed bestrophin-1 suggest a cytosolic function. For example, bestrophin-1 was found to co-localize with stromal interacting molecule-1 (Stim-1), a Ca^{2+} sensor protein in intracellular Ca^{2+} stores [4]. Over-expression of bestrophin-1 in HEK 293 cell line was found to accelerate the speed of Ca^{2+} release from Ca^{2+} stores [5] favoring the idea that bestrophin-1 Cl⁻ channel activities couples the flow of Cl⁻ as counterions to the Ca^{2+} transport in the endoplasmic reticulum (ER) Ca^{2+} store [4]. The role of bestrophin-1 in the ER was supported by analysis of its endogenous localization in RPE cells. After differential centrifugation, bestrophin-1 isolated from freshly isolated porcine RPE cells was found in the same fraction as the ER Cl⁻ channel ClC-3 [31]. Furthermore, levels of resting Ca^{2+} in bestrophin-1 knockout mice appeared to be higher compared to those in wild-type animals and altered patterns of Ca^{2+} release from intracellular stores were reported [31]. In addition, the $Best^{W93C/W93C}$ knock-in mouse model shared properties of Ca^{2+} signaling with that in the knockout mouse, suggesting that mutant bestrophin-1 could have the same effect as the knockout of bestrophin-1 [52]. This is supported by a recent study where several mutated forms at four hot spots in the BEST-1 gene showed cytosolic trafficking defects [29].

The co-localization of bestrophin-1 and Stim-1 suggests a function in intracellular Ca^{2+}-store-dependent Ca^{2+} signaling [4]. Ca^{2+}-store-dependent Ca^{2+} signaling occurs after stimulation of cell surface receptors that generates 1,4,5-inositol-trisphosphate (InsP₃) through activation of phospholipase C (PLC), evokes a biphasic increase in cytosolic free Ca^{2+} concentration [6]. A central mechanism in this

reaction, the store-operated Ca^{2+} entry (SOCE), plays important roles in the regulation of cellular processes such as exocytosis, secretion, phagocytosis, gene regulation, and proliferation [32]. The SOCE activation is enabled by Stim-1 and Ca^{2+}-conducting ion channels in the plasma membrane such as Orai channels or transient receptor potential (TRP) channels [13, 21, 35, 50]. Stim-1, a native ER protein, senses the luminal levels of Ca^{2+} in the store [9]. The depletion of ER Ca^{2+} stores activates Stim-1 and leads to its translocation close to the plasma membrane. This translocation enables the activation of Orai-1 channels by physical interaction with Stim-1 [18] leading to a Ca^{2+} influx from extracellular space into the cell [47]. In the human RPE, the SOCE pathway was found to be mediated by Stim–Orai interaction [12].

In summary, the analysis of bestrophin-1 function revealed contradictory results between data from heterologous expression and animal models with endogenously expressed bestrophin-1. The hypothesis that bestrophin-1 is an intracellular Cl⁻ channel in ER Ca^{2+} stores would combine these conclusions into one model. In order to study this, we used a cell culture model with robust endogenous bestrophin-1 expression and siRNA knockdown of bestrophin-1 to study the contribution of bestrophin-1 in SOCE. We found that knockdown of endogenous bestrophin-1 expression decreases the amount of Ca^{2+} which can be released from intracellular stores after inhibition of sarcoplasmic Ca^{2+}-ATPase (SERCA) and influences SOCE, which characterizes bestrophin-1 as an intracellular protein of the ER.

Material and methods

Cell culture of primary porcine RPE

Eyes were opened through an incision along the *Ora serrata* and the vitreous was removed. Eye cups were incubated with pre-warmed PBS-EDTA (1 mM) for 30 min until the retina was detached and removed. After that, eye cups were incubated again in PBS-EDTA for 30 min followed by incubation in an enzyme solution composed of L-Cys (10×, 260 mM), BSA (100 mg/ml), and Papain (Worthington) for 23 min at 37 °C. The harvest of the RPE was done by suction/pipetting up and down with cell culture medium: 500 ml alpha modification of MEM (Sigma M-4526), fetal calf serum Gold (PAA), 5 ml glut-pen-strep. (Sigma G-1146), 5 ml N1-Supplement (Sigma N-6530), 5 ml non-essential amino acids, THT (hydrocortisone (20 μg/L), taurine (250 mg/L), and triiodo-thyronine (0.013 μg/L)) to stop the activity of the papain. After that, primary porcine RPE cells were washed and plated using 100 μl of fresh culture medium in 12-well plates on 18-mm

ø glass coverslips overnight in a concentration of $1.0–1.2 \times 10^6$ cells per milliliter. This concentration corresponded with the cell density in a monolayer. The first day the medium contained 10 % FCS and next day wells were refilled containing 5 % FCS and were kept under these conditions for all experiments. Cultures were maintained at 37 °C and 5 %CO_2.

RT-PCR

The RPE cells were collected from confluent cultures grown in a 12-well plate. Total RNA was isolated by using RNeasy Micro Kit (Qiagen, Hilden, Germany). The RNA (1 μg) was reverse transcribed with following reaction mixture: 1 μg oligo dT primer (Invitrogen), 1 mM of each dNTP, 20 U RNAguard (Amersham Biosciences), and 20 U M-MLV reverse transcriptase (Invitrogen, Darmstadt, Germany). PCR experiments were performed in 35 cycles, for porcine bestrophin-1(30 s 94 °C, 30 s 56 °C, and 30 s 72 °C) and for porcine Stim-1-2 and porcine Orai1-3 (30 s 94 °C, 30 s 60 °C, and 30 s 72 °C) with 1 μl cDNA in 25-μl PCR reaction mixtures with Taq DNA polymerase (Stratagene), and 1.5 pmol of sense and antisense oligonucleotides specific to various Orai channels and Stim proteins (Table 1).

Real-time quantitative PCR

The total RNA extraction and reverse transcription was performed in the same manner as described for RT-PCR. Quantitative PCR experiments were performed in 45 cycles (5 s 94 °C, 10 s 60 °C, and 2 min 72 °C) for porcine bestrophin-1. It was used 5 μl of cDNA, diluted 1:5 with H_2O in 15-μl PCR reaction mixtures using SsoFastTM Eva-Green® Supermix (*BIO-RAD*), and 1.5 pmol of sense and antisense oligonucleotides specific for porcine bestrophin-1 (Table 1).

Small interfering RNA (siRNA)

Duplexes of 25-nucleotide RNAi were designed and synthesized by Invitrogen (Paisley, UK). Both target and scrambled siRNAs were labeled with Alexa 488 for detection and to establish the optimal transfection condition. In the last step of cell isolation, cells were resuspended in the appropriate medium containing the RNAi duplexes and plated. We used a mixture of three different RNAi duplexes for Orai-1 siRNA and bestrophin-1 siRNA (Table 2).

Ca^{2+} imaging

RPE cells grown on coverslips were washed with Ringer solution (145 mM NaCl, 0.4 mM KH_2PO_4, 1.6 mM K_2HPO_4, 5 mM glucose, 1 mM $MgCl_2 \times 6H_2O$, 1.3 mM Ca-Gluconate$\times 1$ H_2O, pH 7.4, with NaOH) and loaded with Fura-2-AM (Invitrogen) for 45 min in Opti-MEM I containing 6 μM Fura-2 (at 37 °C). Cells were washed again and incubated for 15 min using a Ringer solution. The coverslips were placed into a bath chamber superfused constantly with Ringer solution at 37 °C which was mounted onto the stage of a Zeiss inverted microscope (Axiovert 35, Zeiss, Jena, Germany) equipped with a ×40 Fluar objective. The ratiometric measurements were performed by exciting Fura-2 fluorescence (340/380 nm) at 2-s intervals using a high-speed polychromator system (Visitron Systems, Puchheim, Germany), and the emitted light was filtered with a 510-nm filter and detected by a cooled charge-coupled device camera (CoolSNAP). Data was recorded and analyzed with MetaFlour software and MetaAnalysis software, respectively (both from Universal Imaging Corporation, Puchheim, Germany). In order to calculate intracellular free Ca^{2+} ($[Ca^{2+}]i$), the cells were superfused with the Ringer solution, without Ca^{2+}, with 5 mM EGTA and 2 μM ionomycin. After this, cells were superfused with Ringer solution supplemented

Table 1 Primers used for RT-PCR

Gene	Acc. no.	Sequence	Length
BEST1	AY064707.1	Forward: AGTTTCGAGTTGCTCCCAGA Reverse: ATCAGTCTGGGTAAGGAGGA	212
ORAI1	NM_001173519.1	Forward: GTCAAGTTCTTGCCCCTCA Reverse: CGATAAAGATCAGGCCGAAG	177
ORAI2	NM_001191348.1	Forward: AACTGGTCACCTCCAACCAC Reverse: CTCGCTGATGGAGTTGAGGT	302
ORAI3	NM_001193202.1	Forward: GTCTGCTGCCTCACATTGAA Reverse: ACAAACTTGACCCAGCCAAC	171
STIM1	NM_003156.3	Forward: TGTGGAGCTGCCTCAGTATG Reverse: AAGAGAGGAGGCCCAAAGAG	183
STIM2	NM_020860.3	Forward: CTCTAACACGCCCACCTCAT Reverse: CTTCCTGTGCCTTTTCAAGC	207

Gene	siRNA sequence	Position
BEST1	Sense: CCACACAACUCAUUCUGGAUGCCCU Antisense: AGGGCAUCCAGAAUGAGUUGUGUGG	72
	Sense: CCCUCUUCACGUUCCUGCAGUUCUU Antisense: AAGAACUGCAGGAACGUGAAGAGGG	364
	Sense: CCCAUGGAGCGAGAUAUGUACUGGA Antisense: UCCAGUACAUAUCUCGCUCCAUGGG	534
ORAI1	Sense: CGGUGAGCAAUGUGCACAACCUCAA Antisense: UUGAGGUUGUGCACAUUGCUCACCG	470
	Sense: CCUUUGGCCUGAUCUUUAUCGUCUU Antisense: AAGACGAUAAAGAUCAGGCCAAAGG	764
	Sense: GGGCACUUCAGAGCUUUGGCCUUAA Antisense: UUAAGGCCAAAGCUCUGAAGUGCCC	950

Table 2 Duplexes of 25-nucleotides RNAi labeled with Alexa 488 for the knockdown of bestrophin-1 and Orai-1 protein

with 2 μM ionomycin and saturated Ca^{2+} concentration. $[Ca^{2+}]i$ was calculated according to Grynkiewicz et al. [15]:

$$[Ca^{2+}] = k_d^*(R - R_{min})/(R_{max} - R)^* S_f/S_b$$

Where, R is the fluorescence intensity ratio $[F\,(340)/F\,(380)]$, R_{min} the value where R is minimal (with EGTA) and R_{max} the value when R is maximal (with saturating Ca^{2+} and ionomycin). K_d represents the dissociation constant of Fura-2 (224 nM), and S_f and S_b are the maximum and the minimum fluorescence, respectively, after excitation with 380 nm.

Store-operated calcium entry experiments To activate SOCE, a standard paradigm shown in many previous studies was used [19]: passive release of Ca^{2+} from ER Ca^{2+} stores by inhibition of endoplasmic Ca^{2+} ATPase using 1 μM thapsigargin for 3 min which was followed by application of extracellular Ca^{2+}-free solution for 80 s. After re-addition of extracellular Ca^{2+} to the physiological level after 60 s, a strong increase in intracellular free Ca^{2+} was observed which corresponds with the SOCE.

Immunoprecipitation

Confluent porcine RPE cells were divided into two groups: treated cells with thapsigargin and non-treated cells as control. Non-treated cells were kept in Ringer solution at the same time as the first group (treated cells). The treated group was washed with Ringer for 5 min and later was incubated for 5 min more with thapsigargin (1 μM). Then, the thapsigargin was substituted by Ca^{2+}-free solution for 1 min. Immediately, cells of both groups were lysed in 6-well plate by shaking for 15 min at 4 °C with ice-cold lysis buffer (150 mM Tris–HCl, pH7.5, 150 mM NaCl, 1 % Nonidet-P40, 0.5 % natrium deoxycholate). Cell lysate was scraped and transferred to a new tube and lysed for additional

15 min at 4 °C with rocking. The lysates were clarified by centrifugation at 13,000×g for 10 min at 4 °C.

Pre-clearing

Protein lysates were precleared with 50 μl of Protein G-Agarose (Sigma) and incubated 3 h at 4 °C. After this pre-clearing and centrifugation at 13,000×g for 1 min, the lysates were mixed in new tubes with 50 μl of Protein G-Agarose. This G-Agarose was previously incubated for 1 h with 3 μg of primary antibody against bestrophin-1. The lysates were incubated with the complex of protein G and antibody overnight at 4 °C. Next day, the antibody-coupled protein G was pellet after each wash (three times) by centrifugation (1.200×g for 1 min at 4 °C) with washing buffer. (1) Washing buffer (50 mM Tris–HCl, pH7.5, 150 mM NaCl, 1 % Nonidet-P40, 0.5 % natrium deoxycholate, one tablet Complete Mini protein inhibitor mixture/10 ml (Roche Applied Science), and 0.7 mg/ml pepstatin). (2) Washing buffer (50 mM Tris–HCl, pH7.5, 250 mM NaCl, 0.1 % Nonidet-P40, and 0.05 % natrium deoxycholate). (3) Washing buffer (50 mM Tris–HCl, pH7.5, 50 mM NaCl, 0.1 % Nonidet-P40, and 0.05 % natrium deoxycholate). Protein complexes were dissociated from beads by incubation at 37 °C for 30 min in 4× SDS loading buffer.

Western blotting

Protein extracts from RPE were separated by 10 % SDS-PAGE and transferred to a PVDF membrane, then blocked with buffer (PBS, 0.05 % Tween 20) containing 5 % non-fat dried milk powder for 1 h at room temperature. Membranes were incubated overnight at 4 °C with primary antibodies anti-bestrophin-1 (1:3,000; mouse monoclonal, abcam 2182, , Cambridge, UK), anti-stim-1 (1:1.000; rabbit polyclonal, Santa Cruz Laboratory, USA), anti-Orai-1 (1:300; rabbit polyclonal, Alomone Laboratory, Israel) and anti-β-actin (1:5,000; mouse monoclonal, abcam 6276,

Cambridge, UK) diluted in PBS/Tween and 0.001 % milk (5 % non-fat dried milk powder). After washing the membranes three times for 10 min with PBS/Tween, the membranes were incubated with the appropriate anti-rabbit or anti-mouse IgG HRP-labeled antibody (1:5,000; NEB, Frankfurt, Germany) for 1 h at room temperature. These were then washed again and visualized after 1–3-min incubation with enhanced chemiluminescence (Amersham Pharmacia Biotech, Freiburg, Germany). The experiments were performed three times each.

Transepithelial resistance

Transepithelial electrical resistance (TER) of the porcine RPE monolayer was measured with a volt-ohm meter (World Precision Instruments, Sarasota, USA). Porcine RPE monolayer was grown on Transwell polycarbonate filters (0.4-mm pore size), which contain an insert diameter of 1.2 cm and an effective growth area of 1 cm^2. The upper chamber was filled with 0.5 ml and the lower one filled with 1 ml of pre-warm appropriate RPE medium described before (primary porcine RPE cell isolation). Porcine RPE cells were seeded at a density of 10^6 cells per mmilliliter and were grown to reach a stable TER, representing a confluent monolayer, generally 10 days after seeding. The medium was changed every 3 days. The polycarbonate filters without cells showed as average a TER of 120 Ωcm^2.

Immunocytochemistry

Porcine RPE cells grown on *Transwell* polycarbonate filter or on 18-mm ø cover glass were washed with PBS and immediately fixed with 4 % (*w/v*) paraformaldehyde for 5 min at room temperature. After washing three times with 1× PBS/Tween, porcine RPE cells were permeabilized with a blocking buffer (0.5 % Triton× 100, 10 % goat serum, 1× PBS pH 7.4, distilled H$_2$O) for 30 min. Then the cells were labeled overnight with the primary antibodies: anti-bestrophin-1 (1:500; abcam 2182, mouse monoclonal, Cambridge, UK) or anti-bestrophin-1 (1:500; rabbit polyclonal, provided by Prof. Dr. Karl Kunzelmann, Regensburg University, Germany), anti-stim-1 (1:500; rabbit polyclonal, Santa Cruz Laboratory, USA) and β-catenin (1:500; mouse monoclonal, BD Transduction Laboratories^{TM}) diluted in an antibody buffer (0.1 % Triton×100, 2 % goat serum, 1× PBS pH 7.4, and distilled H$_2$O). Next, after three additional washing steps, cells were incubated for 1 h with appropriate secondary antibodies (conjugated with Alexa Fluor 488 and Cy3; Invitrogen). Single and double immunostainings were mounted and analyzed in an inverted microscope (Observer Z1; Carl Zeiss, Inc.) equipped with a confocal laser scanning microscope (LSM 710; Carl Zeiss, Inc.) operated with the ZEN 2008 software, the polychromatic illumination system

VisiChrome (Visitron), and the MetaMorph software package (Universal Imaging Corp.). The scanning of different channels (488- and 550-nm emission) was performed separately and below saturation levels to avoid crosstalk between chromophores. We used the software package ImageJ for quantitative analysis. Pearson's correlation coefficient (PCC) was calculated to estimate co-localization according to Abramoff [1]. PCC recognizes patterns that match from one image to another describing distribution from pixel histograms in the intensity between the recording channels. PCC cannot compare the pixel intensity values, instead compares only the similarity of shapes between two images. Values of PCC range from −1 to 1. Negative one (−1) indicates no overlap and 1 perfect correlation.

Statistical analysis

[Ca^{2+}]$_I$ data are presented in mean values±SEM. Statistical significance are calculated using the Student's *t* test with *p* values [*$p < 0.05$ (significant), **$p < 0.01$ (highly significant), and ***$p < 0.001$ (extreme highly significant)]. All calculations were performed in Microsoft office Excel 2007 (Microsoft, Munich, Germany).

Results

Endogenously expressed bestrophin-1 localizes to the ER

In order to analyze function and localization of endogenously expressed bestrophin-1, we chose a system that enables reliable identification of porcine RPE cells isolated from live retinas as a model system. We first sought to verify bestrophin-1 expression and find that indeed bestrophin-1 localizes to the basolateral region of RPE cells as expected (Fig. 1a). Next, we confirmed that our RPE dissociation and culturing approach does not alter bestrophin-1 expression, up to 48 h post-dissociation, as determined by immunohistochemistry, western blot analysis, and qPCR (Fig. 1b–d). Thus, RPE cells in short-term cultured porcine retina represent a reliable system to study the function of endogenously expressed bestrophin-1.

To determine intracellular localization of bestrophin-1, we took an immunohistochemical approach in polarized porcine RPE cells grown on filters. These cells reached a transepithelial resistance of 451.7±14.6 Ωcm^2, as shown previously to be a characteristic of healthy RPE cells. Next, polarized porcine RPE cells were immunolabeled against bestrophin-1, Stim-1 (a Ca^{2+}-sensor protein that localizes to the ER membrane), and β-catenin (a non-ER membrane protein as control) (Fig. 2a–c; *n*=3). Pearson's co-localization coefficients were calculated as previously reported by Milenkovic et al. [29] to quantify co-localization patterns of these proteins. The

Fig. 1 Bestrophin-1 in porcine RPE cells. **a** Paraffin section of the porcine retina; *upper left panel*: light micrograph (DIC: differential interference contrast); *upper right panel*: immunostaining of bestrophin-1 (in *red*). **b** Forty-eight-hour cultured primary porcine RPE cells; *lower left panel*: light micrograph (DIC); *lower right panel*: immunostaining of bestrophin-1 (in *red*). **c** Expression of bestrophin-1 protein in porcine RPE cells after 24-, 48-, and 72-h isolation. **d** Expression of *BEST1* gene in porcine RPE cells after 24-, 48-, and 72-h isolation
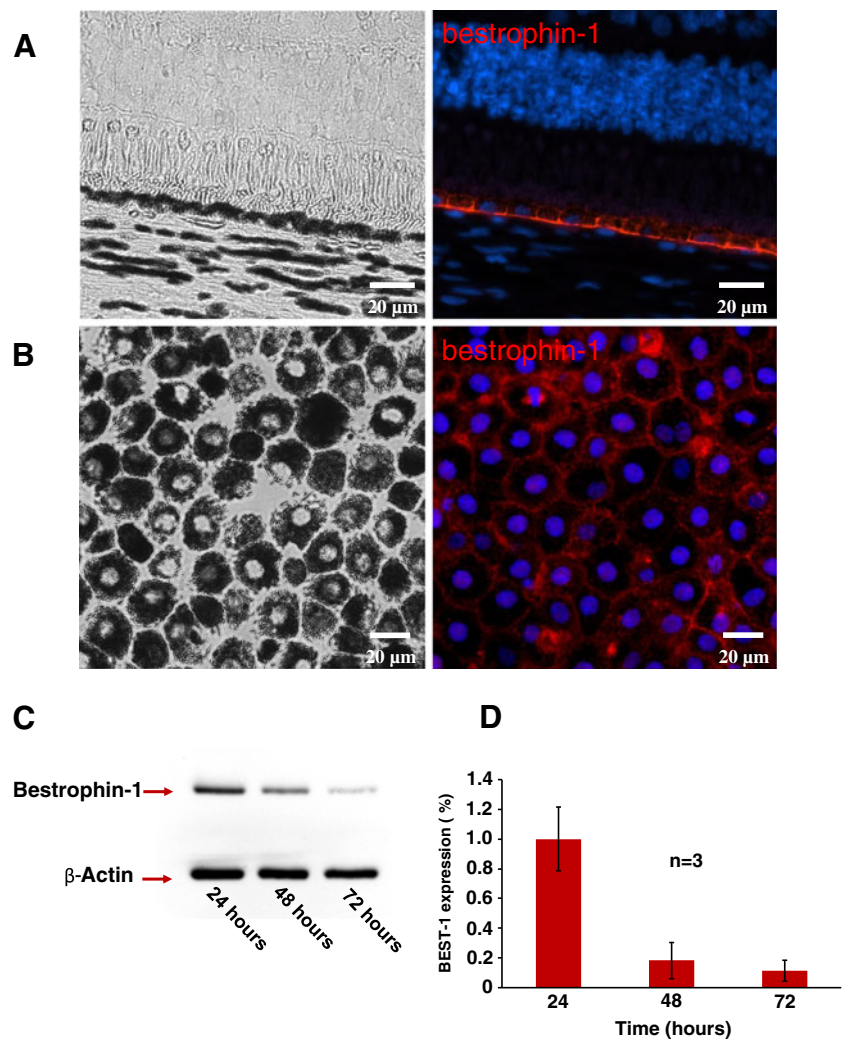
coefficient describes co-localization on a scale from −1 to +1, such that +1 indicates complete co-localization and −1 complete non-localization. Based on this scale we find that Stim-1 and β-catenin, which are expressed in physically distinct cellular structures, have a co-localization coefficient of 0.22± 0.001. In comparison, we find a significantly higher co-localization coefficient between bestrophin-1 and Stim-1 (0.44±0.0013), whereas bestrophin-1/ β-catenin is not significantly different than stim-1/β-catenin negative control (0.25± 0.006) (Fig. 2d, $n=10$; $p\leq0.001$). Based on these results, we argue that bestrophin-1 is enriched in the ER membrane.

Store-operated calcium entry is mediated by Orai-1 in porcine RPE cells

We next asked whether bestrophin-1 localization to the ER membrane is required for proper store-operated Ca^{2+} entry (SOCE) in porcine RPE cells. As an initial step, we verified the expression of know SOCE components in porcine RPE cells in two ways. (1) Using RT-PCR (Fig. 3a), we were able

to detect mRNA expression of Icrac channels ORAI-1, 2, 3 and STIM-1, 2. (2) Although antibodies exist for only stim-1 and orai-1, we were able to detect both by Western blot analysis (Fig. 3b).

The contribution of these proteins to SOCE in RPE cells was first investigated by means of pharmacological intervention. For these experiments, we used a two-step SOCE manipulation paradigm (Fig. 3c). In the first step (SOCE1), we activated SOCE as described previously [19]. Briefly, we used the ER Ca^{2+}-ATPase antagonist thapsigargin in combination with Ca^{2+}-free extracellular solution (for 80s) to reduce intracellular Ca^{2+} levels. After reintroduction of Ca^{2+} to the extracellular solution, we observed after 60 s a strong increase in intracellular free Ca^{2+} (i.e., SOCE). In the second step (SOCE2), we first waited for a maximum SOCE response from step1 (i.e., maximum internal Ca^{2+} level), then we repeated the first step but in the absence of thapsigargin. Since thapsigargin is an irreversible blocker of endoplasmic Ca^{2+}-ATPase, depleted ER Ca^{2+} levels will not be replenished even after Ca^{2+} is reintroduced to the external buffer.
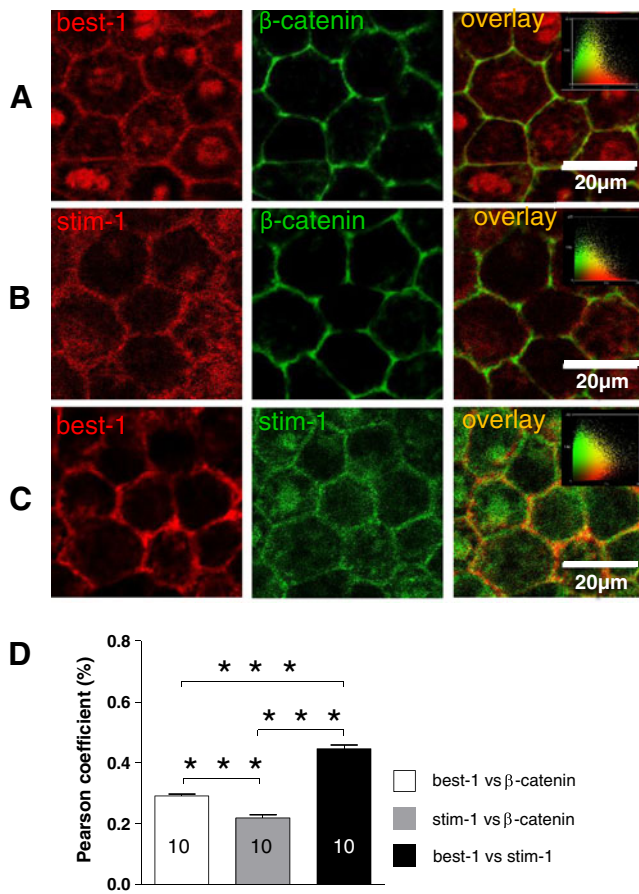
Fig. 2 Confocal microscopy of polarized porcine RPE cells on filter Porcine RPE cells were directly isolated from the eye and seeded on filters and used for immunocytochemistry when the transepithelial electrical resistance was above 400 Ωcm^2. **a** *Upper left panel*: immunostaining of bestrophin-1 (in *red*); *upper center panel*: immunostaining of β-catenin (in *green*), and *upper right panel*: overlay of both proteins. **b** *Middle left panel*: immunostaining of Stim-1 (in *red*), *middle center panel*: immunostaining of β-catenin (in *green*), and *middle right panel*: overlay of both proteins. **c** *Lower left panel*: immunostaining of bestrophin-1 (in *red*), *lower center panel*: immunostaining of Stim-1 (in *green*), and *lower right panel*: overlay of both proteins. **d**: Pearson's co-localization analysis between bestrophin-1, Stim-1, and β-catenin were calculated on the base of the pixel histograms shown in the *inserts* of the *right panels* [1]. A coefficient of +1 indicates complete co-localization. (*** $P \leq 0{,}001$; $n = 10$ per group; these experiments were replicated three times)

Therefore, increased internal Ca^{2+} concentration associated with SOCE must be originated from extracellular Ca^{2+} compartment rather than ER stores. This also means that after SOCE1, no Ca^{2+} should be taken up into the ER. Thus it is likely that ion channel blockers applied at SOCE2 will not interfere with the interaction between of Ca^{2+} stores and only influence Ca^{2+} channels in the plasma membrane.

In order to test whether TRP channels are involved in SOCE, we used the TRP and voltage-gated Ca^{2+} channel antagonist SKF96365 [38]. Importantly, we observed that in the absence of pharmacological manipulation SOCE1 and
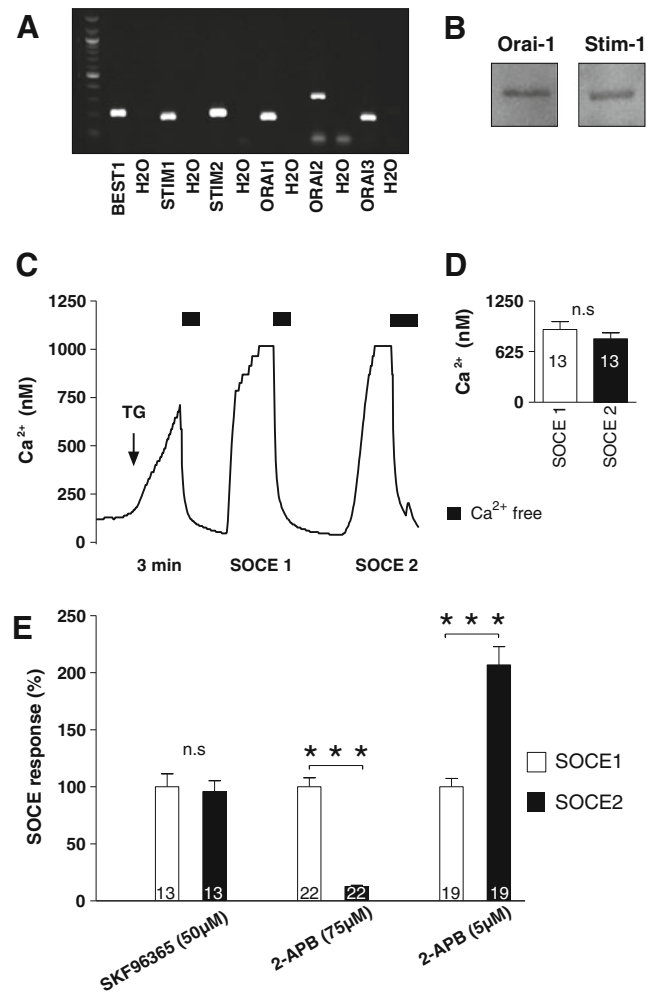

Fig. 3 Store-operated calcium entry (SOCE) in porcine RPE cells. **a** After RNA isolation from 48-h cultivated primary porcine RPE cells, RT-PCR showed the expression of *BEST1* and the genes involved in SOCE: *STIM1*, *STIM2*, *ORAI*, *ORAI2*, and *ORAI3*. **b** Western blots showing the presence of Stim-1 and Orai-1 proteins. **c** SOCE activation using the double paradigm in porcine RPE ($n = 13$); cells were first treated with Ringer solution until the resting Ca^{2+} stabilized. After that, cells were treated with thapsigargin (1 μM) for 3 min and followed by the application of a Ca^{2+}-free solution for 80 s. Then, ringer solution was re-added to the cells. After 2 min of SOCE activation peak, Ca^{2+}-free solution was re-added for 80 s and again followed by the re-addition of Ringer solution, keeping this second SOCE activation peak for 2 min again. **d** Statistic analysis of the SOCE in the double paradigm ($n = 13$; n.s.). Using the double paradigm experiment, it was possible to take the first SOCE activation peak (SOCE1) as a control for further experiments. **e** Effects of different SOCE agonist/antagonist drugs. Using the double paradigm experiment in porcine RPE cells, all drugs were applied in the second SOCE activation peak (SOCE2). From the *left* to the *right*: SKF96365 (50 μM) did not show any effect ($n = 13$; n.s), 2-APB (75 μM) was highly significant ($n = 22$; $p \leq 0.001$) as well as 2-APB (5 μM; $n = 19$; $p \leq 0.001$)

SOCE2 are not significantly different (amplitude of SOCE1 = 898.6 ± 98.2 nM and of SOCE2 = 785.4 ± 73.5 nM; $n = 13$), suggesting they can be used for direct comparison (Fig. 3d). Application of SKF96365 during SOCE2 in RPE cells did not lead

to a significant difference in SOCE amplitudes as compared to SOCE1 (Fig. 3e; $n=13$). 2-Aminoethoxydiphenyl borate (2-APB) is known to have unique pharmacological effects on Orai channels depending on its concentration: application of 2-APB at high concentrations inhibits and at low concentrations potentiates Orai channel activation [37]. 2-APB used at a high concentration (75 μM) reduced SOCE2 by 87.3 ± 7.6 % compared to the SOCE1 control ($n=22$; $p\leq0.001$; Fig. 3e).We next tested low 2-APB concentration, but surprisingly did not observe an increased SOCE response. One possible explanation is that low 2-APB cannot further activate Orai channels due to a saturated SOCE response. To address this, we retested the response to low 2-APB concentration on SOCE activation in the absence of thapsigargin, in which passive release of Ca^{2+} from stores was achieved simply by application of extracellular Ca^{2+}-free bath solution as we have previously published. [11]. Under these conditions, 2-APB (5 μM) enhanced SOCE2 by 106 ± 14.6 % compared to the control SOCE1 (Fig. 3e; $n=19$; $p\leq0.001$).

The pharmacological data suggest that Orai channel activation is involved in SOCE. To directly test if the Orai channel is required for SOCE, we used siRNA-mediated knockdown of Orai-1. We observed that treatment of RPE cells with Orai-1 siRNA significantly reduced Orai-1 protein levels (Fig. 4a, b). We next compared SOCE activation between cells treated with Orai-1 siRNA ($n=82$) and in control cells which were transfected with non-specific (scrambled) siRNA ($n=86$). The SOCE amplitude was significantly reduced by 65.2 % in cells treated with Orai-1 siRNA compared to control cells: amplitude of $SOCE_{Orai-1\ siRNA}=174.4\pm22.1$ nM and amplitude of $SOCE_{scrambled}=500.7\pm31.51$ nM (Fig. 4c and d; $p\leq0.001$).

Bestrophin-1 influences store-operated calcium entry in porcine RPE cells

Based on our observation that bestrophin-1 localizes to the ER, we next tested whether bestrophin-1 is required for SOCE by taking an siRNA knockdown approach (bestsiRNA). We find that bestrophin-1 protein levels in RPE cells are reduced by greater than 80 % after siRNA treatment, as assayed by densitometric analysis of Western
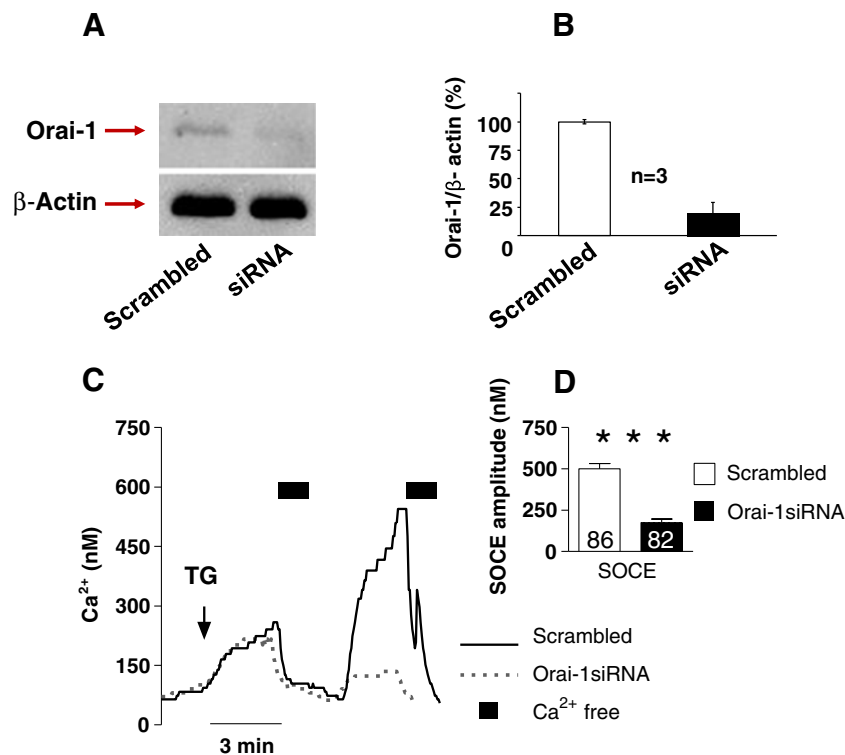

Fig. 4 Knockdown of Orai-1 protein. **a** Western blot shows the knockdown of Orai-1 protein in Orai-1 siRNA-transfected cells compared to scrambled-transfected cells. Equal amounts of protein were loaded to the blot. This experiment was replicated three times. **b** Densitometric quantification of Orai-1 knockdown. **c** Calcium tracing of scrambled (*solid line*) and Orai-1 siRNA (*dashed line*)-transfected porcine RPE cells showing the effect of knockdown Orai-1 protein in the SOCE activation amplitude. Cells were treated first with Ringer solution, after thapsigargin (1 μM) was applied for 3 min and followed by Ca^{2+}-free solution for 1 min, and later, extracellular Ca^{2+} was re-added to the cells. **d** Statistic analysis of SOCE activation amplitude in scrambled against to Orai-1 siRNA-transfected cells (***$P\leq0,001$; $n_{scrambled}=86$ and $n_{siOrai-1}=82$; all experiments were done in three different rounds of primary cells isolation; number of scrambled experiments=8, and number of Orai-1 siRNA experiments=6)

blots (Fig. 5a–b). However, the expression Orai-1 and Stim-1 proteins was not changed by treatment with bestrophin-1 siRNA (Fig. 5a)

As mentioned above, bestrophin-1 showed some co-localization with Stim-1. Thus we investigated whether bestrophin-1 is involved in SOCE by means of bestrophin-1 RNAi approach. We performed two analyses to determine the effect of best-1 knockdown. First, we measured SOCE in cells transfected with scrambled siRNA as compared to

cells transfected with best-1 siRNA. Second, in order to identify siRNA-transfected cells and therefore to directly compare siRNA-transfected cells with non-transfected controls in one Ca^{2+}-imagining experiment, siRNAs were labeled with alexa 488 (Fig. 5d). We measured best-1 siRNA-transfected cells versus non-transfected cells in the same recording. Thus the effect of bestrophin-1 knockdown ($n=90$) was investigated against three controls: scrambled siRNA ($n=86$), non-transfected controls during investigation of scrambled siRNA
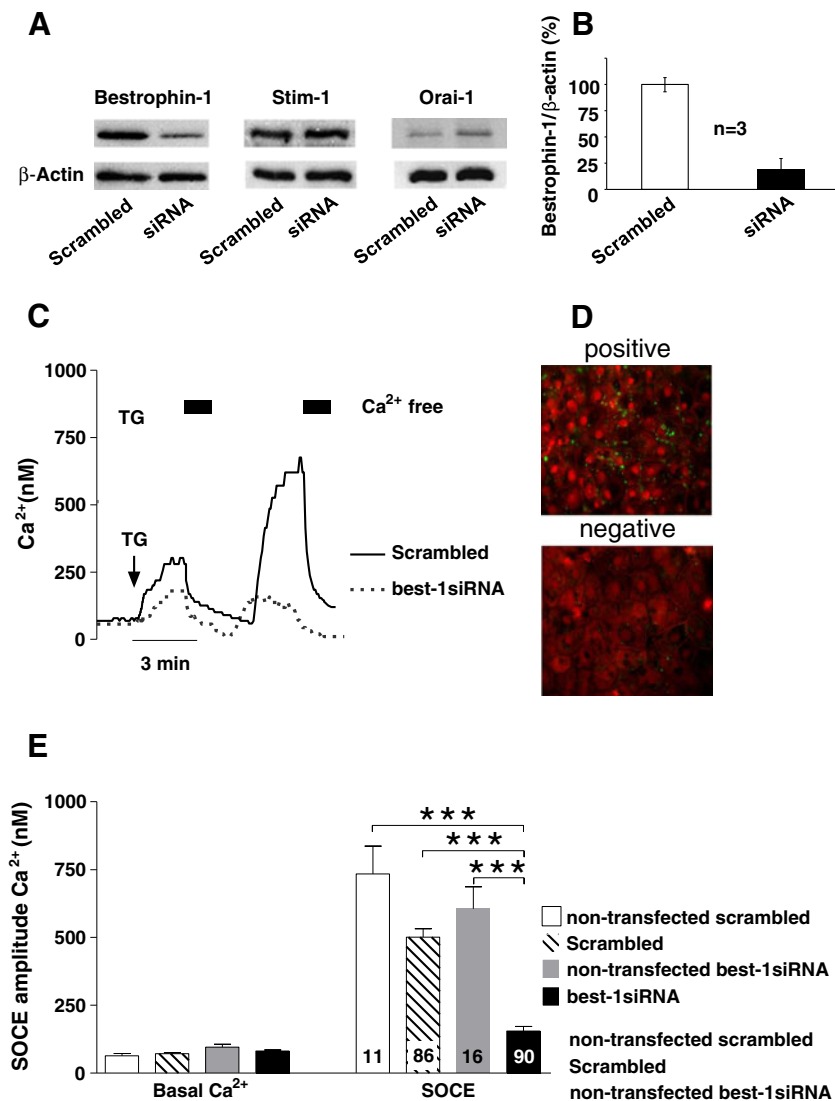

Fig. 5 Knockdown of bestrophin-1 protein. **a** Western blot shows the knockdown of bestrophin-1 protein in best-1 siRNA-transfected cells compared to scrambled siRNA-transfected cells. Stim-1 and Orai-1 proteins did not show any expression changes levels due to Best-1 siRNA. Equal amounts of protein were loaded to the blot. **b** Quantification of knockdown bestrophin-1 after a densitometric analysis. **c** Calcium tracing of SOCE in scrambled (*solid line*) and Best-1 siRNA-transfected (*dashed line*) cells. Cells were treated previously with Ringer solution, after thapsigargin (1 μM) was applied for 3 min and followed by Ca^{2+}-free solution for 80 s, and later, extracellular Ca^{2+} was re-added to the cells. **d** Detection of best-1 siRNA-transfected cells. Cells transfected (*upper panel*) and not transfected (*lower panel*) with Alexa 488 fluorophor-labeled best-1 siRNA. **e** Statistic analysis of basal Ca^{2+} and SOCE activation amplitude between scrambled siRNA- and best-1 siRNA-transfected cells. Transfected cells and non-transfected (n.t) cells were also compared within each set of experiment (Best-1 siRNA and scrambled; *$P \leq 0{,}05$; **$P \leq 0{,}01$; ***$P \leq 0{,}001$; $n_{scrambled}=86$ and $n_{scrambled(n.t)}=11$; $n_{best-1\ siRNA}=90$ and $n_{best-1\ siRNA(n.t)}=16$; all experiments were done in three different rounds of primary cells isolation; number of scrambled experiment=8, and number of Best-1 siRNA experiment=6)

($n=11$), and non-transfected controls during investigation of best-1 siRNA ($n=16$) (Fig. 5e).

We find that cells treated with best-1 siRNA showed a ~70 % decrease in SOCE amplitude as compared to that observed in non-transfected cells or cells transfected with scrambled siRNA. SOCE amplitude in cells treated with bestrophin-1 siRNA was reduced by 69.1 % compared to that in the three different controls: amplitude of $SOCE_{best-1\ siRNA}=155.01\pm17.06$ nM versus amplitude in $SOCE_{scrambled}=500.7\pm31.5$ nM, versus amplitude $SOCE_{scrambled(n.t)}=734.22\pm102.67$ nM in non-transfected cells of scrambled siRNA experiments and amplitude $SOCE_{best-1\ siRNA(n.t)}=605.85\pm81.27$ nM in non-transfected cells of bestrophin-1 siRNA experiments (Fig. 5d, e; $p\leq0.001$).

We next sought to determine if bestrophin-1 and Stim-1 interact during SOCE. As mentioned above, best-1 siRNA does not alter Orai-1 or Stim-1 expression, and therefore reduced Orai-1 and Stim-1 expression cannot explain the observed reduction in SOCE amplitude (Fig. 5a). Barro-Soria et al. [4] reported that bestrophin-1 and Stim-1 proteins physically interact under overexpression conditions, suggesting that the reduced SOCE amplitude might result from reduced bestrophin-1/Stim-1 interaction. Although we found co-localization of bestrophin-1 and Stim-1 in immune histochemistry, it does not prove whether these proteins also interact when endogenously expressed. Thus we attempted to confirm a physical interaction between endogenously expressed bestrophin-1 and Stim-1 by means of immunoprecipitation experiments; however, we were unable to co-immunoprecipitate these proteins in either cells under control conditions or cells which had been treated by the protocol to induce SOCE. These results suggest that they do not physically interact under endogenous conditions (Fig. 6).

To further address the mechanism underlying reduced SOCE amplitude after knockdown of bestrophin-1 expression, we next measured the amplitude of Ca^{2+} released from ER stores after application of two distinct SERCA pump inhibitors (Fig. 7a–b). First, we applied cyclopiazonic acid (CPA) under physiological extracellular Ca^{2+} conditions. Here, we found that cells treated with best-1 siRNA showed a significantly dampened increase in Ca^{2+} release amplitude as compared to control cells: $CPA_{best-1\ siRNA}=292.73\pm23.18$ and $CPA_{scrambled}=364.95\pm19.36$: (Fig. 7a; $p\leq0.05$). In addition, this finding was supported in SOCE experiments in which the application of thapsigargin showed a remarkable reduction of Ca^{2+} amplitude in those cells treated with best-1 siRNA compared to control cells: $Ca^{2+}thapsi_{best-1\ siRNA}=100.21$ nM±6.40 and $Ca^{2+}thapsi_{scrambled}=290.10$ nM±18.25 (Fig. 7; $p\leq0.001$). This reduction was also significant as compared to non-transfected controls: amplitude $thapsi_{scrambled(n.t)}=317.09\pm58.47$ nM in scrambled siRNA experiments and amplitude $thapsi_{best-1\ siRNA(n.t)}=206.58\pm$
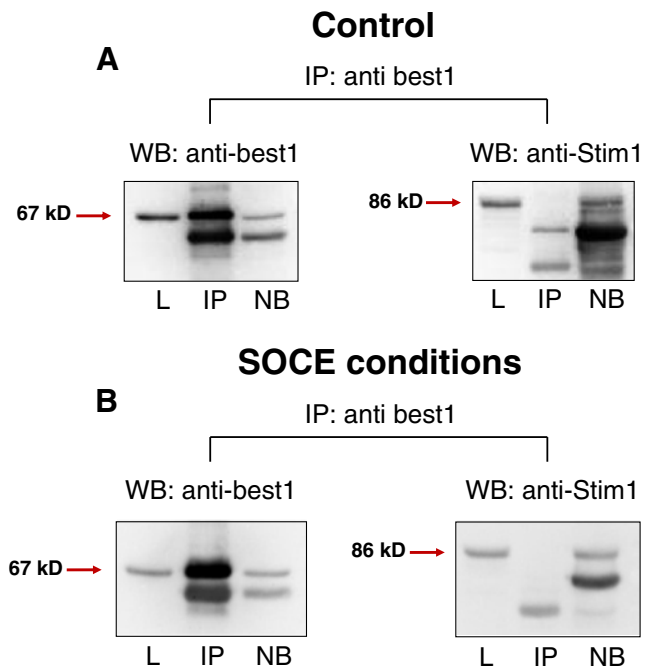

Fig. 6 Immunoprecipitation and co-immunoprecipitation of bestrophin-1 and Stim-1, respectively, in treated and non-treated porcine RPE cells. **a** In non-treated cells in resting conditions, no interaction between bestrophin-1 and Stim-1 proteins could be detected. **b** Also in cells in which SOCE activation has been performed no functional interaction bestrophin-1 and Stim-1 proteins was detected. ($L=$ lysate; $NB=$ non-bound fraction after immunoprecipitation; $IP=$ immunoprecipitates)

15.37 nM in bestrophin-1 siRNA experiments (Fig. 7b; $p\leq0.001$).

Because of the strong reduction in the amplitude of the Ca^{2+} response observed in cells treated with best-1 siRNA after SERCA inhibition, we hypothesized that the SOCE response depends on the amount of Ca^{2+} released from stores. To test this, we determined the total amount of Ca^{2+} released upon SERCA inhibition by thapsigargin. In agreement with our hypothesis, best-1 siRNA-treated cells showed a 67.1 ± 5.9 % reduction in Ca^{2+} released from ER stores as compared to that of scrambled and Orai-1 siRNA groups. In contrast, neither scrambled nor Orai-1 siRNA-treated cells showed significant differences between the amounts of Ca^{2+} released from ER stores (Fig. 7c; $p\leq0.001$).

Discussion

The present work reveals that a sizeable proportion of endogenously expressed bestrophin-1 is localized intracellularly to the ER. Furthermore, we provide evidence that bestrophin-1 is required for the activation of SOCE and functions in the same pathway as Orai-1 protein and Stim-1. These conclusions are based on the following findings:
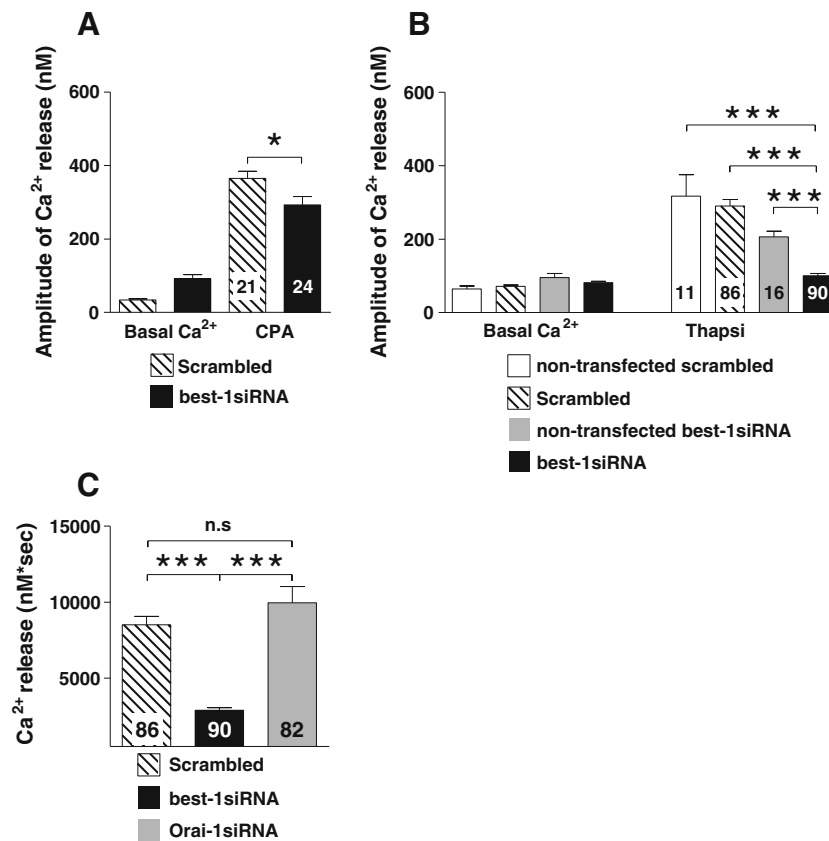
Fig. 7 Comparison of Ca^{2+} release from cytosolic stores in response to application of different SERCA pump inhibitors. **a** Statistic analysis of the amplitude of Ca^{2+} release by application of cyclopiazonic acid between scrambled and best-1 siRNA-transfected cells (***$P \leq 0.001$; $n_{scrambled}=21$ and $n_{best-1\ siRNA}=24$). **b** Statistic analysis of the amplitude of Ca^{2+} release by application of thapsigargin between scrambled and best-1 siRNA-transfected cells. Transfected cells and non-transfected (n.t.) cells were also compared inside each group (best-1 siRNA and scrambled; *$P \leq 0.05$; **$P \leq 0.01$; ***$P \leq 0.001$; $n_{scrambled}=86$ and $n_{scrambled(n.t)}=11$; $n_{best-1\ siRNA}=90$ and $n_{best-1\ siRNA(n.t)}=16$). **c** Statistical analysis of the amount of Ca^{2+} release by application of thapsigargin between scrambled, best-1 siRNA and Orai-1 siRNA. The Ca^{2+} release was quantified by integration of the area below the curve of Ca^{2+} increases during thapsigargin (1 μM) application. In every experiment, thapsigargin was applied for 3 min (***$P \leq 0.001$; $n_{scrambled}=86$, $n_{best-1\ siRNA}=90$, and $n_{Orai-1\ siRNA}=82$)

(1) endogenously expressed bestrophin-1 co-localizes with the ER Ca^{2+}-sensor protein Stim-1; (2) siRNA knockdown of Orai-1 expression significantly reduces SOCE amplitude; (3) siRNA knockdown of bestrophin-1 expression led to: (a) a decrease in the amount of calcium released from ER stores after SERCA inhibition and (b) a decrease in SOCE amplitude.

Most studies to date focused on bestrophin-1 function were performed under bestrophin-1 overexpression conditions. The aim of this study was to investigate the function of endogenously expressed bestrophin-1. We used a 48-h porcine RPE cell culture model that showed characteristics similar to native RPE. These cells, grown on filters, reached transepithelial resistances of more than 400 Ωcm^2, and exhibited high levels of endogenous bestrophin-1 expression localized to the basolateral membrane. Importantly, bestrophin-1 protein levels reduced by best-1 siRNA, further confirmed the specifity of the anti-bestrophin-1 antibody used in this study here.

Endogenously expressed bestrophin-1 localizes to ER Ca^{2+} stores

To investigate the subcellular localization of endogenously expressed bestrophin-1 in polarized RPE cells, pixel analysis of immunohistochemical stainings against bestrophin-1, Stim-1 (a Ca^{2+}-sensing proteins of ER Ca^{2+} stores), and β-catenin (a marker for plasma membrane localization) was used. We found that bestrophin-1 co-localized with Stim-1; because Stim-1 interact with Orai-1 channels in the plasma membrane, we conclude that the intracellular localization of bestrophin-1 must be very close to the basolateral membrane. Indeed, we showed in a recent study that after differential centrifugation, bestrophin-1 co-precipitates with an intracellular Cl^- channel (ClC-3) in fresh porcine RPE cells [31]. Furthermore, we show here that bestrophin-1 is distinctly localized from β-catenin and cadherin in the basolateral membrane of porcine retina [31]. This observation is in agreement

with similar subcellular localization findings for bestrophin-1 in lung epithelial cells [4].

Orai-1 is involved in SOCE activation in porcine RPE cells

Our analysis of the endogenous bestrophin-1 expression pattern suggests that it is localized to the ER Ca^{2+} stores that contain Stim-1. As a part of our investigation, we provided evidence that the role of Orai-1 antagonist/agonist (2-APB) altered the SOCE response, while the voltage-gated Ca^{2+} channel antagonist (SKF96365) had no effect. Since the effects of ion channel blockers were studied in a repeated SOCE activation paradigm, the blocker could only affect the ion channels and not the Stim-1/Orai-1 mechanism. Furthermore, we provided evidence that siRNA knockdown of Orai-1 led to reduce Orai-1 protein levels and reduced SOCE amplitude. This is in agreement with previous findings, in which the activation of TRP channels or Orai channels was found to provide the underlying Ca^{2+} entry pathway in SOCE. Recently, we showed that the ARPE-19 cell line displays SOCE activation mediated by Orai channels [12]. One potential caveat to our approach is that we used an aggressive and artificial and direct depletion of Ca^{2+} stores with strong gradients to induce SOCE. The endogenous physiological pathway, which involves the activation of G-protein coupled receptor, is likely more moderate.

Bestrophin-1 influences the SOCE pathway in porcine RPE cells

To determine if bestrophin-1 functions in the porcine RPE SOCE pathway, we took three approaches. First, we analyzed the bestrophin-1 expression pattern and found that it localized to the ER Ca^{2+} stores that contain Stim-1. Next, we demonstrated that siRNA knockdown of bestrophin-1 results in reduced SOCE amplitude (similar to reduced Orai-1). One possible explanation for this phenotype is based on a finding that under overexpression conditions, bestrophin-1 and Stim-1 physically interact. However, we found no physical interaction of endogenously expressed bestrophin-1 and Stim-1, arguing against this explanation. Furthermore, these results suggest that although we report here that bestrophin-1 and Stim-1 exhibit similar subcellular localization by immunohistochemically, they do not physically interact or do so weakly.

If the reduction in SOCE associated with decreased bestrophin-1 expression cannot be explained by a bestrophin-1/Stim-1 interaction, what might be the cause? A hint for a possible underlying mechanism is the observation that the rise in intracellular Ca^{2+} associated with the SOCE response is significantly dampened under best-1 knockdown conditions as compared to controls. Based on this observation, we measured the amount of Ca^{2+} released from cytosolic Ca^{2+} stores in response to treatment by

thapsigargin under extracellular Ca^{2+} conditions. [8]. We found that cells treated with best-1 siRNA showed a large reduction in the amount of Ca^{2+} released from stores compared to that from the corresponding control cells: treated with scrambled siRNA or treated with Orai-1 siRNA. Thus, the reduction in Ca^{2+} amplitude induced by SOCE activation is at least partially due to a reduction in the amount of Ca^{2+} released from the ER. These data fit nicely with the current model for the SOCE, in which Orai-1 channels in the plasma membrane are activated through an interaction with Stim-1 in ER Ca^{2+}-stores [47]. Stim-1 itself is activated by the release of Ca^{2+} from cytoplasmic stores. Here, we provide evidence that in RPE cells treated with best-1 siRNA, less Ca^{2+} is release from internal stores. This in turn could lead to reduced Stim-1 and Orai-1 activation and ultimately to a decreased SOCE response. This model is supported by a recent study in which the authors found that bestrophin-1 modulates calcium release from ER stores after application of thapsigargin or CPA [5]. For example, in HEK cells overexpressing human bestrophin-1, application of CPA trigged Ca^{2+} release from ER stores faster than in control cells [5]. In addition, we showed in a previous study that in RPE cells from $Best1^{-/-}$ mice, ATP-induced Ca^{2+} signals were generated by different Ca^{2+} stores than those in $Best1^{+/+}$ animals [31]. However, the effects of loss of bestrophin-1 function in mouse models have an added confound because bestrophin-1 exhibits strong developmental expression [3] and likely leads to secondary, so far unknown changes in RPE differentiation.

That there is less Ca^{2+} release in cells with reduced bestrophin-1 expression fits well with the idea that bestrophin-1 is an intracellular Ca^{2+}-dependent Cl^- channel [17]. In this function, bestrophin-1 would conduct the counterion for the transport activity of the Ca^{2+}-ATPase in the ER, SERCA. Since bestrophin-1 Cl^- channel function is Ca^{2+} dependent, bestrophin-1 would further enhance SERCA pump activity when intracellular Ca^{2+} concentration is high. Furthermore, bestrophin-1 functioning as a Ca^{2+}-dependent Cl^- channel would facilitate the release of Ca^{2+} from stores after activation of inositol-1,4,5-trisphosphate-receptor. Here, the Ca^{2+} dependence would provide a feed-forward loop to accelerate the Ca^{2+} release [4]. In accordance with this, we found that cells with reduced bestrophin-1 expression showed slightly elevated resting $[Ca^{2+}]_I$ compared to that in corresponding controls. This is in agreement with a similar finding in which RPE cells from bestrophin-1 knockout mice also exhibit elevated resting $[Ca^{2+}]_I$ [31].

Taken together, our histological analysis and functional analysis of SOCE support a model in which endogenously expressed bestrophin-1 is at least partly an intracellular Ca^{2+}-dependent Cl^- channel. The functional analysis suggests that bestrophin-1 conducts the counterion for Ca^{2+} transport in and out of cytosolic Ca^{2+} stores. This conclusion leads us to a

model that integrates the observations made in both the over-expression systems [17], which identified bestrophin-1 as a Cl^- channel, and in the bestrophin-1 animal models, which revealed no contribution of endogenously expressed bestrophin-1 to the RPE Cl^- conductance [23, 52]. Further-more, the intracellular bestrophin-1 function can be easily combined with its function as an L-type Ca^{2+} channel regulator [28, 49]. The intracellular localization of bestrophin-1 in Stim-1-containing ER Ca^{2+} stores is close enough so that the C-terminus of bestrophin-1 can interact with L-type channels that are found in the RPE basolateral membrane [34]. Since L-type channels increase intracellular free Ca^{2+} the bestrophin-1/L-type channel interaction would link L-type activity with Ca^{2+} uptake into ER Ca^{2+} store and therefore store-dependent Ca^{2+} signaling which has been reported for rat RPE cells [27].

Our results presented here and the observations of recent publications do not exclude the possibility that there is a small proportion of bestrophin-1 in the plasma membrane as has been described in overexpression systems. Since a pro-portion of bestrophin-1 was found intracellularly with over-expression [4, 39, 43], one possibility is that bestrophin-1 physiologically localizes to both the ER membrane and the plasma membrane. An alternative possibility is that bestrophin-1 is shuttled between the ER and the plasma membrane, an expression pattern that is common among many Cl^- channels [20, 25]. However, under resting con-ditions, the majority of bestropin-1 would be localized in the ER. This would explain why in RPE cells from bestrophin-1 knockout mice or transgenic mice carrying the W93C mu-tation, which is known to lead to a loss of bestrophin-1, Cl^- channel function shows no differences in Cl^- conductance as compared to that of wild-type mice.

Increased cytosolic free Ca^{2+} modulates many cellular processes in the RPE such as secretion, gene expression, phagocytosis, and transepithelial transport [45]. Mutations of bestrophin-1 lead to Best's vitelliforme macular dystro-phy [24], an autosomal dominant inherited form of macular degeneration associated with a strong lipofuscin accumula-tion in the RPE [44]. One possibility is that mutant bestrophin-1 changes the Ca^{2+}-dependent regulation of RPE function [42]. The proper regulation of RPE function would require the basolateral localization as we have de-scribed here. Indeed, mutated BEST1 gene, including those observed in Best patients [30], has been shown to exhibit reduced peripheral localization. This is due to mutant bestrophin-1 not trafficking to the periphery of the cell, where it functions as a Cl^- channel [29]. The periphery of the cell is the region where the ER Ca^{2+} stores are involved in SOCE. Thus, we should expect reduced activation of SOCE in cells that express mutant bestrophin-1 as well. This is in accordance with findings in a Best's disease mouse model [51]. The knock-in mouse carrying a W93C mutation in bestrophin-1 showed reduced ATP-stimulated

Ca^{2+} signals and older animals show signs of retinal degeneration [51]. The reduced Ca^{2+}-signals in the $Best1^{W93C/W93C}$ mice could result from a loss of intra-cellular Cl^- channel function and/or from reduced bestrophin-1 trafficking. In following this idea, it is likely that mutant bestrophin-1 also affects SOCE in human patients. Therefore our finding opens a new route to understand how mutant bestrophin-1 can mod-ulate calcium homeostasis in RPE.

References

1. Abramoff MD, Magelhaes PJ, Ram SJ, Zhang S, Campochiaro PA, Zack DJ, Hughes BA (2004) Image processing with image. J Biophotonics Int 11(2):36ß42
2. Arden GB, Barrada A, Kelsey JH (1962) New clinical test of retinal function based upon the standing potential of the eye. Br J Ophthalmol 46(8):449–467
3. Bakall B, Marmorstein LY, Hoppe G, Peachey NS, Wadelius C, Marmorstein AD (2003) Expression and localization of bestrophin during normal mouse development. Invest Ophthalmol Vis Sci 44(8):3622–3628
4. Barro Soria R, Spitzner M, Schreiber R, Kunzelmann K (2009) Bestrophin-1 enables Ca2+-activated Cl^- conductance in epithelia. J Biol Chem 284(43):29405–29412. doi:10.1074/jbc.M605716200
5. Barro-Soria R, Aldehni F, Almaca J, Witzgall R, Schreiber R, Kunzelmann K (2010) ER-localized bestrophin 1 activates Ca2+-dependent ion channels TMEM16A and SK4 possibly by acting as a counterion channel. Pflugers Arch 459(3):485–497. doi:10.1007/s00424-009-0745-0
6. Berridge MJ (1993) Inositol trisphosphate and calcium signalling. Nature 361(6410):315–325. doi:10.1038/361315a0
7. Bok D (1993) The retinal pigment epithelium: a versatile partner in vision. J Cell Sci Suppl 17:189–195
8. Brandman O, Liou J, Park WS, Meyer T (2007) STIM2 is a feedback regulator that stabilizes basal cytosolic and endoplasmic reticulum Ca2+ levels. Cell 131(7):1327–1339. doi:10.1016/j.cell.2007.11.039
9. Cahalan MD, Zhang SL, Yeromin AV, Ohlsen K, Roos J, Stauderman KA (2007) Molecular basis of the CRAC channel. Cell Calcium 42(2):133–144. doi:10.1016/j.ceca.2007.03.002
10. Constable PA (2011) Nifedipine alters the light-rise of the electro-oculogram in man. Graefes Arch Clin Exp Ophthalmol 249(5):677–684. doi:10.1007/s00417-010-1604-6
11. Cordeiro S, Strauss O (2010) Expression of Orai genes and I (CRAC) activation in the human retinal pigment epithelium. Graefes Arch Clin Exp Ophthalmol 249(1):47–54. doi:10.1007/s00417-010-1445-3
12. Cordeiro S, Strauss O (2011) Expression of Orai genes and I (CRAC) activation in the human retinal pigment epithelium. Graefes Arch Clin Exp Ophthalmol 249(1):47–54. doi:10.1007/s00417-010-1445-3
13. Feske S, Gwack Y, Prakriya M, Srikanth S, Puppel SH, Tanasa B, Hogan PG, Lewis RS, Daly M, Rao A (2006) A mutation in Orai1 causes immune deficiency by abrogating CRAC channel function. Nature 441(7090):179–185. doi:10.1038/nature04702
14. Gal A, Li Y, Thompson DA, Weir J, Orth U, Jacobson SG, Apfelstedt-Sylla E, Vollrath D (2000) Mutations in MERTK, the human orthologue of the RCS rat retinal dystrophy gene, cause retinitis pigmentosa. Nat Genet 26(3):270–271. doi:10.1038/81555

15. Grynkiewicz G, Poenie M, Tsien RY (1985) A new generation of Ca2+ indicators with greatly improved fluorescence properties. J Biol Chem 260(6):3440–3450

16. Gu SM, Thompson DA, Srikumari CR, Lorenz B, Finckh U, Nicoletti A, Murthy KR, Rathmann M, Kumaramanickavel G, Denton MJ, Gal A (1997) Mutations in RPE65 cause autosomal recessive childhood-onset severe retinal dystrophy. Nat Genet 17 (2):194–197. doi:10.1038/ng1097-194

17. Hartzell HC, Qu Z, Yu K, Xiao Q, Chien LT (2008) Molecular physiology of bestrophins: multifunctional membrane proteins linked to best disease and other retinopathies. Physiol Rev 88 (2):639–672. doi:10.1152/physrev.00022.2007

18. Hogan PG, Lewis RS, Rao A (2010) Molecular basis of calcium signaling in lymphocytes: STIM and ORAI. Annu Rev Immunol 28:491–533. doi:10.1146/annurev.immunol.021908.132550

19. Hoth M, Penner R (1992) Depletion of intracellular calcium stores activates a calcium current in mast cells. Nature 355(6358):353–356. doi:10.1038/355353a0

20. Jentsch TJ, Maritzen T, Zdebik AA (2005) Chloride channel diseases resulting from impaired transepithelial transport or vesicular function. J Clin Invest 115(8):2039–2046. doi:10.1172/JCI25470

21. Liou J, Kim ML, Heo WD, Jones JT, Myers JW, Ferrell JE Jr, Meyer T (2005) STIM is a Ca2+ sensor essential for Ca2+-store-depletion-triggered Ca2+ influx. Curr Biol 15(13):1235–1241. doi:10.1016/j.cub.2005.05.055

22. Marmorstein AD, Marmorstein LY, Rayborn M, Wang X, Hollyfield JG, Petrukhin K (2000) Bestrophin, the product of the Best vitelliform macular dystrophy gene (VMD2), localizes to the basolateral plasma membrane of the retinal pigment epithelium. Proc Natl Acad Sci U S A 97(23):12758–12763. doi:10.1073/pnas.220402097

23. Marmorstein LY, Wu J, McLaughlin P, Yocom J, Karl MO, Neussert R, Wimmers S, Stanton JB, Gregg RG, Strauss O, Peachey NS, Marmorstein AD (2006) The light peak of the electroretinogram is dependent on voltage-gated calcium channels and antagonized by bestrophin (best-1). J Gen Physiol 127(5):577–589. doi:10.1085/jgp.200509473

24. Marquardt A, Stohr H, Passmore LA, Kramer F, Rivera A, Weber BH (1998) Mutations in a novel gene, VMD2, encoding a protein of unknown properties cause juvenile-onset vitelliform macular dystrophy (Best's disease). Hum Mol Genet 7(9):1517–1525

25. Martins JR, Kongsuphol P, Sammels E, Dahimene S, Aldehni F, Clarke LA, Schreiber R, de Smedt H, Amaral MD (1812) Kunzelmann K F508del-CFTR increases intracellular Ca(2+) signaling that causes enhanced calcium-dependent Cl(−) conductance in cystic fibrosis. Biochim Biophys Acta 11:1385–1392. doi:10.1016/j.bbadis.2011.08.008

26. Maw MA, Kennedy B, Knight A, Bridges R, Roth KE, Mani EJ, Mukkadan JK, Nancarrow D, Crabb JW, Denton MJ (1997) Mutation of the gene encoding cellular retinaldehyde-binding protein in autosomal recessive retinitis pigmentosa. Nat Genet 17 (2):198–200. doi:10.1038/ng1097-198

27. Mergler S, Strauss O (2002) Stimulation of L-type Ca(2+) channels by increase of intracellular InsP3 in rat retinal pigment epithelial cells. Exp Eye Res 74(1):29–40. doi:10.1006/exer.2001.1128S0014483501911285

28. Milenkovic VM, Krejcova S, Reichhart N, Wagner A, Strauss O (2011) Interaction of bestrophin-1 and Ca2+ channel beta-subunits: identification of new binding domains on the bestrophin-1 C-terminus. PLoS One 6(4):e19364. doi:10.1371/journal.pone.0019364PONE-D-10-05789

29. Milenkovic VM, Rohrl E, Weber BH, Strauss O (2011) Disease-associated missense mutations in bestrophin-1 affect cellular trafficking and anion conductance. J Cell Sci 124(Pt 17):2988–2996. doi:10.1242/jcs.085878

30. Mullins RF, Oh KT, Heffron E, Hageman GS, Stone EM (2005) Late development of vitelliform lesions and flecks in a patient with best disease: clinicopathologic correlation. Arch Ophthalmol 123 (11):1588–1594. doi:10.1001/archopht.123.11.1588

31. Neussert R, Muller C, Milenkovic VM, Strauss O (2010) The presence of bestrophin-1 modulates the Ca2+ recruitment from Ca2+ stores in the ER. Pflugers Arch 460(1):163–175. doi:10.1007/s00424-010-0840-2

32. Parekh AB (2010) Store-operated CRAC channels: function in health and disease. Nat Rev Drug Discov 9(5):399–410. doi:10.1038/nrd3136

33. Petrukhin K, Koisti MJ, Bakall B, Li W, Xie G, Marknell T, Sandgren O, Forsman K, Holmgren G, Andreasson S, Vujic M, Bergen AA, McGarty-Dugan V, Figueroa D, Austin CP, Metzker ML, Caskey CT, Wadelius C (1998) Identification of the gene responsible for Best macular dystrophy. Nat Genet 19(3):241–247. doi:10.1038/915

34. Reichhart N, Milenkovic VM, Halsband CA, Cordeiro S, Strauss O (2010) Effect of bestrophin-1 on L-type Ca2+ channel activity depends on the Ca2+ channel beta-subunit. Exp Eye Res 91 (5):630–639. doi:10.1016/j.exer.2010.08.001

35. Roos J, DiGregorio PJ, Yeromin AV, Ohlsen K, Lioudyno M, Zhang S, Safrina O, Kozak JA, Wagner SL, Cahalan MD, Velicelebi G, Stauderman KA (2005) STIM1, an essential and conserved component of store-operated Ca2+ channel function. J Cell Biol 169(3):435–445. doi:10.1083/jcb.200502019

36. Rosenthal R, Bakall B, Kinnick T, Peachey N, Wimmers S, Wadelius C, Marmorstein A, Strauss O (2006) Expression of bestrophin-1, the product of the VMD2 gene, modulates voltage-dependent Ca2+ channels in retinal pigment epithelial cells. FASEB J 20(1):178–180. doi:10.1096/fj.05-4495fje

37. Schindl R, Bergsmann J, Frischauf I, Derler I, Fahrner M, Muik M, Fritsch R, Groschner K, Romanin C (2008) 2-Aminoethoxydiphenyl borate alters selectivity of Orai3 channels by increasing their pore size. J Biol Chem 283(29):20261–20267. doi:10.1074/jbc.M803101200

38. Singh A, Hildebrand ME, Garcia E, Snutch TP (2010) The transient receptor potential channel antagonist SKF96365 is a potent blocker of low-voltage-activated T-type calcium channels. Br J Pharmacol 160(6):1464–1475. doi:10.1111/j.1476-5381.2010.00786.x

39. Stanton JB, Goldberg AF, Hoppe G, Marmorstein LY, Marmorstein AD (2006) Hydrodynamic properties of porcine bestrophin-1 in Triton X-100. Biochim Biophys Acta 1758(2):241–247. doi:10.1016/j.bbamem.2006.01.024

40. Steinberg RH (1985) Interactions between the retinal pigment epithelium and the neural retina. Doc Ophthalmol 60(4):327–346

41. Strauss O (2005) The retinal pigment epithelium in visual function. Physiol Rev 85(3):845–881. doi:10.1152/physrev.00021.2004

42. Sun H, Tsunenari T, Yau KW, Nathans J (2002) The vitelliform macular dystrophy protein defines a new family of chloride channels. Proc Natl Acad Sci U S A 99(6):4008–4013. doi:10.1073/pnas.05269299999/6/4008

43. Tsunenari T, Sun H, Williams J, Cahill H, Smallwood P, Yau KW, Nathans J (2003) Structure-function analysis of the bestrophin family of anion channels. J Biol Chem 278(42):41114–41125. doi:10.1074/jbc.M306150200M306150200

44. Weingeist TA, Kobrin JL, Watzke RC (1982) Histopathology of Best's macular dystrophy. Arch Ophthalmol 100(7):1108–1114

45. Wimmers S, Karl MO, Strauss O (2007) Ion channels in the RPE. Prog Retin Eye Res 26(3):263–301. doi:10.1016/j.preteyeres.2006.12.002

46. Wu J, Marmorstein AD, Striessnig J, Peachey NS (2007) Voltage-dependent calcium channel CaV1.3 subunits regulate the light peak of the electroretinogram. J Neurophysiol 97(5):3731–3735. doi:10.1152/jn.00146.2007

47. Yeromin AV, Zhang SL, Jiang W, Yu Y, Safrina O, Cahalan MD (2006) Molecular identification of the CRAC channel by altered ion selectivity in a mutant of Orai. Nature 443(7108):226–229. doi:10.1038/nature05108

48. Yu K, Qu Z, Cui Y, Hartzell HC (2007) Chloride channel activity of bestrophin mutants associated with mild or late-onset macular

degeneration. Invest Ophthalmol Vis Sci 48(10):4694–4705. doi:10.1167/iovs.07-0301

49. Yu K, Xiao Q, Cui G, Lee A, Hartzell HC (2008) The best disease-linked Cl⁻ channel hBest1 regulates Ca V 1 (L-type) Ca2+ channels via src-homology-binding domains. J Neurosci 28(22):5660–5670. doi:10.1523/JNEUROSCI.0065-08.2008

50. Zhang Y, Stanton JB, Wu J, Yu K, Hartzell HC, Peachey NS, Marmorstein LY, Marmorstein AD Suppression of Ca2+ signaling in a mouse model of Best disease. Hum Mol Genet 19 (6):1108–1118. doi:10.1093/hmg/ddp583

51. Zhang Y, Stanton JB, Wu J, Yu K, Hartzell HC, Peachey NS, Marmorstein LY, Marmorstein AD (2010) Suppression of Ca2+ signaling in a mouse model of Best disease. Hum Mol Genet 19 (6):1108–1118. doi:10.1093/hmg/ddp583

52. Zhang SL, Yeromin AV, Zhang XH, Yu Y, Safrina O, Penna A, Roos J, Stauderman KA, Cahalan MD (2006) Genome-wide RNAi screen of Ca(2+) influx identifies genes that regulate Ca(2+) release-activated Ca(2+) channel activity. Proc Natl Acad Sci U S A 103(24):9357–9362. doi:10.1073/pnas.0603161103